

Research Paper

Myeloid-specific blockade of Notch signaling ameliorates nonalcoholic fatty liver disease in mice

Jian Ding*, Ming Xu*, Wei Du*, Zhi-Qiang Fang, Hao Xu, Jing-Jing Liu, Ping Song, Chen Xu, Zhi-Wen Li, Zhen-Sheng Yue, Yu-Wei Ling, Juan-Li Duan, Kai-Shan Tao[✉], Fei He[✉], Lin Wang[✉]

Department of Hepatobiliary Surgery, Xi-Jing Hospital, Fourth Military Medical University, Xi'an 710032, China.

* These authors contributed equally to this study.

✉ Corresponding authors: Kai-Shan Tao (taokashan0686@163.com), Fei He (hefei_hefei@163.com, ORCID: <https://orcid.org/0000-0001-8368-5030>) and Lin Wang (fierywang@163.com)© The author(s). This is an open access article distributed under the terms of the Creative Commons Attribution License (<https://creativecommons.org/licenses/by/4.0/>). See <http://ivyspring.com/terms> for full terms and conditions.

Received: 2022.10.23; Accepted: 2023.03.05; Published: 2023.03.27

Abstract

Rationale: Macrophages play a central role in the development and progression of nonalcoholic fatty liver disease (NAFLD). Studies have shown that Notch signaling mediated by transcription factor recombination signal binding protein for immunoglobulin kappa J region (RBP-J), is implicated in macrophage activation and plasticity. Naturally, we asked whether Notch signaling in macrophages plays a role in NAFLD, whether regulating Notch signaling in macrophages could serve as a therapeutic strategy to treat NAFLD.

Methods: Immunofluorescence staining was used to detect the changes of macrophage Notch signaling in the livers of human patients with NAFLD and choline deficient amino acid-defined (CDAA) diet-fed mice. *Lyz2-Cre RBP-J^{fllox}* or wild-type C57BL/6 male mice were fed with CDAA or high fat diet (HFD) to induce experimental steatohepatitis or steatosis, respectively. Liver histology examinations were performed using hematoxylin-eosin (H&E), Oil Red O staining, Sirius red staining and immunohistochemistry staining for F4/80, Col1 α 1 and α SMA. The expression of inflammatory factors, fibrosis or lipid metabolism associated genes were evaluated by quantitative reverse transcription (qRT)-PCR, Western blot or enzyme-linked immunosorbent assay (ELISA). The mRNA expression of liver samples was profiled by using RNA-seq. A hairpin-type decoy oligodeoxynucleotides (ODNs) for transcription factor RBP-J was loaded into bEnd.3-derived exosomes by electroporating. Mice with experimental NAFLD were treated with exosomes loading RBP-J decoy ODNs via tail vein injection. *In vivo* distribution of exosomes was analyzed by fluorescence labeling and imaging.

Results: The results showed that Notch signaling was activated in hepatic macrophages in human with NAFLD or in CDAA-fed mice. Myeloid-specific RBP-J deficiency decreased the expression of inflammatory factors interleukin-1 beta (IL1 β) and tumor necrosis factor alpha (TNF α), attenuated experimental steatohepatitis in mice. Furthermore, we found that Notch blockade attenuated lipid accumulation in hepatocytes by inhibiting the expression of IL1 β and TNF α in macrophages *in vitro*. Meanwhile, we observed that tail vein-injected exosomes were mainly taken up by hepatic macrophages in mice with steatohepatitis. RBP-J decoy ODNs delivered by exosomes could efficiently inhibit Notch signaling in hepatic macrophages *in vivo* and ameliorate steatohepatitis or steatosis in CDAA or HFD mice, respectively.

Conclusions: Combined, macrophage RBP-J promotes the progression of NAFLD at least partially through regulating the expression of pro-inflammatory cytokines IL1 β and TNF α . Infusion of exosomes loaded with RBP-J decoy ODNs might be a promising therapy to treat NAFLD.

Keywords: nonalcoholic fatty liver disease; macrophage; Notch signaling; RBP-J; exosomes; transcription factor decoy

Introduction

Nonalcoholic fatty liver disease (NAFLD), has become the most common type of chronic liver disease, affecting more than a quarter of the world's population [1-3]. NAFLD varies from hepatic steatosis

characterized by accumulation of triglycerides in hepatocytes to nonalcoholic steatohepatitis (NASH), which might progress to fibrosis, cirrhosis and hepatocellular carcinoma [1-3]. However, the mole-

cular mechanisms of NAFLD has not been fully understood, and there are still limited appropriate drugs specifically to treat NAFLD.

Hepatic macrophages, the largest population of innate immune cells in the liver, which account for about 80% of the total macrophages in the body [4, 5]. Hepatic macrophages play a critical role in the maintenance of liver homeostasis and in the development of liver disease, including NAFLD [6-8]. There are two known functional subsets of macrophages: classically activated “pro-inflammatory” M1 macrophages and alternatively activated “anti-inflammatory” M2 macrophages [9, 10]. In NAFLD, macrophages of a pro-inflammatory phenotype seem to contribute to disease severity [7, 10]. High-fat diet (HFD)-fed mice had increased numbers of liver macrophages with preponderant production of pro-inflammatory cytokines [11]. Zhang et al. [12] found that macrophage p38 α causes M1 polarization, and deficiency of macrophage p38 α attenuates experimental steatohepatitis in mice. On the other hand, M2 macrophages with an anti-inflammatory phenotype have been associated with attenuated hepatic injury and insulin resistance in NAFLD [11, 13]. These findings indicate that the development of NAFLD are closely related to the activation of macrophages, especially M1 macrophages, and regulating macrophage activation may be an important strategy for the treatment of NAFLD.

Notch signaling mediated by RBP-J, the transcription factor transactivated by signals from four mammalian Notch receptors [14], is implicated in macrophage activation [15-17]. Notch signaling is required for lipopolysaccharide (LPS)-stimulated macrophage activation through interferon regulatory factor 8 (IRF-8) [17] and nuclear factor κ -light-chain-enhancer of activated B cells (NF- κ B) [18]. We have previously shown that Notch blockade in macrophages could impair the expression of inflammatory factors interleukin-1 beta (IL1 β) and tumor necrosis factor alpha (TNF α) by up-regulation of cylindromatosis (Cyd), and then ameliorate hepatic fibrosis in mice [19]. Therefore, we speculated that inhibition of Notch signaling in macrophages may ameliorate NAFLD.

In this study, we showed that myeloid-specific RBP-J deficiency attenuated experimental steatohepatitis in mice, and the infusion of exosomes loaded with RBP-J decoy ODNs could represent a promising therapeutic strategy for the treatment of NAFLD.

Materials and Methods

Mice

Mice were maintained in a specific pathogen-free (SPF) condition on the C57BL/6 background.

Lyz2-Cre RBP-J^{fllox} mice were donated by Professor Han in Fourth Military Medical University. Littermates (Lyz2-Cre RBP-J^{fllox/+}) were used as the control of Lyz2-Cre RBP-J^{fllox/flox} mice (RBP-J KO). C57BL/6 wild type mice were purchased from Gempharmatech Co., Ltd. (Nanjing, China). To induce experimental NAFLD, male mice (7-8 weeks of age) were fed with choline deficient amino acid-defined diet (CDAA, L-amino acid diet with 45% kcal% fat with 0.1% methionine no added choline, Research Diets, New Brunswick, NJ, USA) for 10 weeks, or high-fat diet (HFD, rodent diet with 60 kcal% fat, Research Diets) for 22 weeks. All animal experiments were performed following the guidelines of the Animal Experiment Administration Committee of Fourth Military Medical University.

Human liver samples

Paraffin embedded liver tissues were obtained from the Department of Hepatobiliary Surgery of Xijing Hospital, Fourth Military Medical University. Liver samples were obtained from seven patients with NASH. Six control individuals had no history of diabetes, alcohol use, or viral hepatitis. All participants had signed informed consents for the use of their samples. The basic information of the patients is listed in Table S1. The protocols involving human samples were approved by the Ethics Committee of Xijing Hospital, Fourth Military Medical University.

Histological analysis

Liver specimens were fixed with 10% buffered formalin or 4% paraformaldehyde (PFA). Formalin-fixed specimens were embedded in paraffin, sectioned, and routinely stained with hematoxylin and eosin (H&E). PFA-fixed samples were embedded with the compound at the optimal cutting temperature (OCT) and sectioned at 8- μ m thickness. The presence of steatosis was confirmed using oil red O staining frozen liver sections. Liver sections were stained with freshly prepared saturated oil red O solution (Servicebio, Wuhan, China) according to standard procedures. Immunofluorescence (IF) and immunohistochemical (IHC) staining were described previously [20].

Biochemistry and Enzyme-linked immunosorbent assay (ELISA)

Serum albumin, alanine aminotransferase (ALT), aspartate aminotransferase (AST), low density lipoprotein (LDL), and triglyceride (TG) levels were determined using an automatic biochemical analyzer (Rayto Life and Analytical Sciences Company, Shenzhen, China).

The levels of IL1 β and TNF α in serum or culture supernatants were measured using kits from Thermo

Fisher Scientific (MA, USA) following the manufacturer's protocols.

Cell culture

Mouse brain endothelial cell line bEnd.3 cells or RAW264.7 macrophages were cultured in DMEM supplemented with 10% fetal bovine serum (FBS), 2 mM L-glutamine, 100 U/ml penicillin and 100 µg/ml streptomycin at 37°C in a 5% CO₂ incubator. AML12 hepatocytes were cultured in DMEM/F-12 (1:1) medium supplemented with 10% FBS, 1% ITS Liquid Media Supplement (Sigma, I3146), Dexamethasone (40 ng/ml) and antibiotics.

Hepatic macrophages were isolated by using magnetic bead cell sorting (MACS) as described [19,20]. Hepatic macrophages cultured with the fresh medium containing lipopolysaccharide (LPS, 100 ng/ml) for 24 h. RAW264.7 macrophages were treated with γ-secretase inhibitor N-[N-(3,5-Difluorophenacetyl)-L-alanyl]-S-phenylglycine t-butyl Ester (DAPT, 5 µM, Selleck Biotechnology Co. LTD, USA) or DMSO for 72 h, changed and cultured with the fresh medium containing LPS for 24 h, and the conditioned medium (CM) were harvested. Next, AML12 hepatocytes were cultured in palmitic acid (PA, 10 mM, Kunchuang Science and Technology Development Co. LTD, Xi'an) medium with CM for 48 h. Then AML12 cells were stained with oil red O (Servicebio). Triglyceride content in AML12 cells was measured using a detection kit (Pulai Biological Co. LTD, Beijing) following the manufacturer's protocols.

Isolation, identification and labeling of Exosomes

Mouse endothelial cell line bEnd.3 was cultured in FBS-free medium for 48 hours. Exosomes in supernatants were isolated using PEG6000 (Sigma) as described [20, 21]. The size distribution of exosomes was analyzed by Laser Scattering Microscopy for nanoparticle tracking analysis (NTA), and the morphology of exosomes was observed by transmission electron microscopy (TEM) in Dolaimi Biotechnology Co., Ltd. (Wuhan, China).

To label exosomes, exosomes in PBS were incubated with DiI (Invitrogen) for 30 min at 37 °C according to the protocol, then washed and centrifuged with PBS containing 12% PEG6000 at 12000 × g for 30 min.

Western blot

Liver tissues, bEnd.3 cells or exosomes were lysed with radioimmunoprecipitation assay (RIPA) buffer (Beyotime) containing phenylmethylsulfonyl fluoride (PMSF, 10 mM), and the protein concentration was quantified using the BCA Protein Assay Kit (Thermo Fisher Scientific, Rockford, IL,

USA) following the manufacturer's instructions. The samples were analyzed by sodium dodecyl sulfate-polyacrylamide gel electrophoresis (SDS-PAGE), transferred to polyvinylidene fluoride (PVDF) membranes (Millipore, Billerica, MA, USA), and incubated with primary antibodies targeting IL1β, TNFα, CD9, Alix, Flotillin-1, and VDAC1 and then with HRP-conjugated goat anti-mouse or anti-rabbit IgG secondary antibodies. The information of the antibodies used is listed in Table S2.

RBP-J decoy ODN loading and exosome injection

We have reported a hairpin RBP-J decoy ODNs in reference [20]. In brief, two RBP-J binding sites (CGTGGGAA [22]) were present in this decoy, with three phosphorothioatemodified sites at each end, whereas the control decoy was introduced mutation in the RBP-J binding sites. The sequence of RBP-J decoy ODNs was 5'-CTGCGTGGGAACTAGCGTGGGAATATTTTTTATATTCCCACGCTAGTCCCA CGCAG-3'; the sequence of the control decoy ODNs was 5'-CTGCGTTTTAACTAGCGTTTTAATATTTTT TATATTAACGCTAGTTAAACGCAG-3'. All the ODNs were synthesized by Tsingke Biotechnology Co. Ltd. (Beijing, China). The decoy ODNs were resuspended at a concentration of 20 µM, incubated for 10 minutes at 95°C, then cooled down to room temperature slowly.

Exosomes were electroporated with decoy ODNs at 400 V and 125 µF in 0.4-cm electroporation cuvettes as previously described [20, 23].

For *in vivo* exosome tracking, CDAA-fed mice were injected with DiI-labeled exosomes via the tail vein. Tissues were harvested 6 h after injection for bioluminescence imaging (Andor iKon Dw434, Oxford Instruments, Oxon, UK) or tissue sectioning.

For exosome-mediated therapy, exosomes were loaded with decoy ODNs and infused into CDAA-fed mice in the 9th and 10th week or those with HFD-fed mice in 21st and 22nd week four times by tail vein injection. Mice were humanely euthanized for further analysis 2-3 days after the last exosome injection.

RNA extraction and quantitative reverse transcription PCR (qRT-PCR)

Total RNA was isolated from liver tissues, hepatic macrophages, RAW264.7 macrophages or AML12 hepatocytes with Trizol reagent (Invitrogen) according to the manufacturer's instructions. The mRNA was reverse transcribed into cDNA using the Evo M-MLV RT Premix (Accurate Biology, China). qRT-PCR was performed with the SYBR Green Premix Pro Taq HS qPCR Kit (Accurate Biology, China) in a Bio -Rad CFX Maestro 2.2 Real-Time PCR

System (Bio-Rad, Hercules, CA, USA). β -actin or GAPDH was served as the internal control. All primers were purchased from Tsingke Biotechnology Co. Ltd. (Beijing, China). The sequences of the primers used are listed in Table S3.

Statistical analysis

Data were analyzed with Graph Pad Prism software, version 8.0. Comparisons between groups were undertaken using unpaired or paired Student's *t*-test. Some data that did not comply with normal distribution were analyzed by the Mann-Whitney test. The number of repetitions were indicated in the legends of each graph. Results were expressed as means \pm SD. $P < 0.05$ was considered as significant.

Results

Notch signaling was activated in hepatic macrophages in human with NASH or in CDAA-fed mice

We examined the expression of Hes1, a key downstream gene of Notch signaling [14], in the liver tissues of patients with NASH and normal controls. As determined by Western blot and immunofluorescence staining, Hes1 expression was significantly higher in patients with NASH than in normal controls, and CD68⁺ hepatic macrophages

mainly co-located with Hes1⁺ cells on liver sections (Fig. S1A,B, Fig. 1B).

We then detected the expression of Notch signaling related genes in livers of wild-type mice fed with CDAA for 10 weeks by qRT-PCR. The mRNA levels of almost all Notch ligands, Notch receptors, target genes Hes1 and Hey1 were significantly up-regulated in liver samples of CDAA-fed mice (Fig. 1E). The protein level of Hes1 was also significantly higher in the livers of CDAA-fed mice than chow-fed mice (Fig. S1C,D). Immunofluorescence staining further showed that Hes1 was up-regulated and co-localized with F4/80⁺ hepatic macrophages in the livers of CDAA-mice (Fig. 1D). These results suggested that Notch signaling was activated in hepatic macrophages during NAFLD progression.

Myeloid-specific RBP-J deficiency attenuated experimental steatohepatitis in CDAA-fed mice

We investigated the role of macrophage Notch signaling in the development of steatohepatitis. RBP-J^{lox} mice were crossed with Lyz2-Cre transgenic mice to obtain myeloid-specific RBP-J knockout (KO) and control mice. The efficiency of RBP-J deletion in liver macrophages was confirmed by qRT-PCR of genomic DNA as described [19]. Myeloid-specific RBP-J KO and control mice were fed with CDAA diet for 10 weeks.

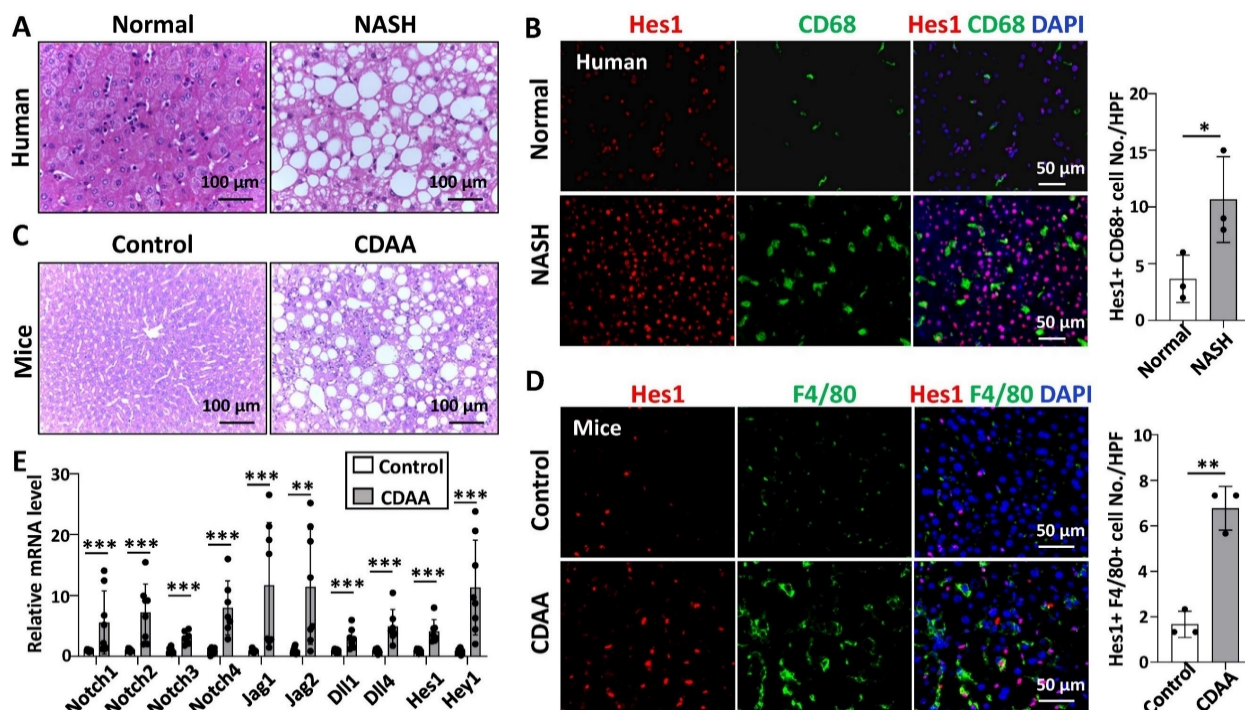


Figure 1. Notch signaling in hepatic macrophages was activated in human with NASH or in CDAA-fed mice. (A) H&E staining of liver tissues from normal or patients with NASH. (B) Immunofluorescence staining for Hes1 and macrophage marker CD68 in liver tissues from normal or patients with NASH, nuclei were counterstained with DAPI, and Hes1⁺ CD68⁺ were quantified and compared. (C) H&E staining of liver tissues in chow-fed or CDAA-fed mice. (D) Immunofluorescence staining for Hes1 and F4/80 in liver tissues from chow-fed or CDAA-fed mice, and Hes1⁺ F4/80⁺ were quantified. (E) The mRNA levels of Notch ligands, Notch receptors, and downstream genes in liver extracts from chow-fed or CDAA-fed mice were determined by qRT-PCR. Bars = means \pm SD; * $P < 0.05$, ** $P < 0.01$, *** $P < 0.001$.

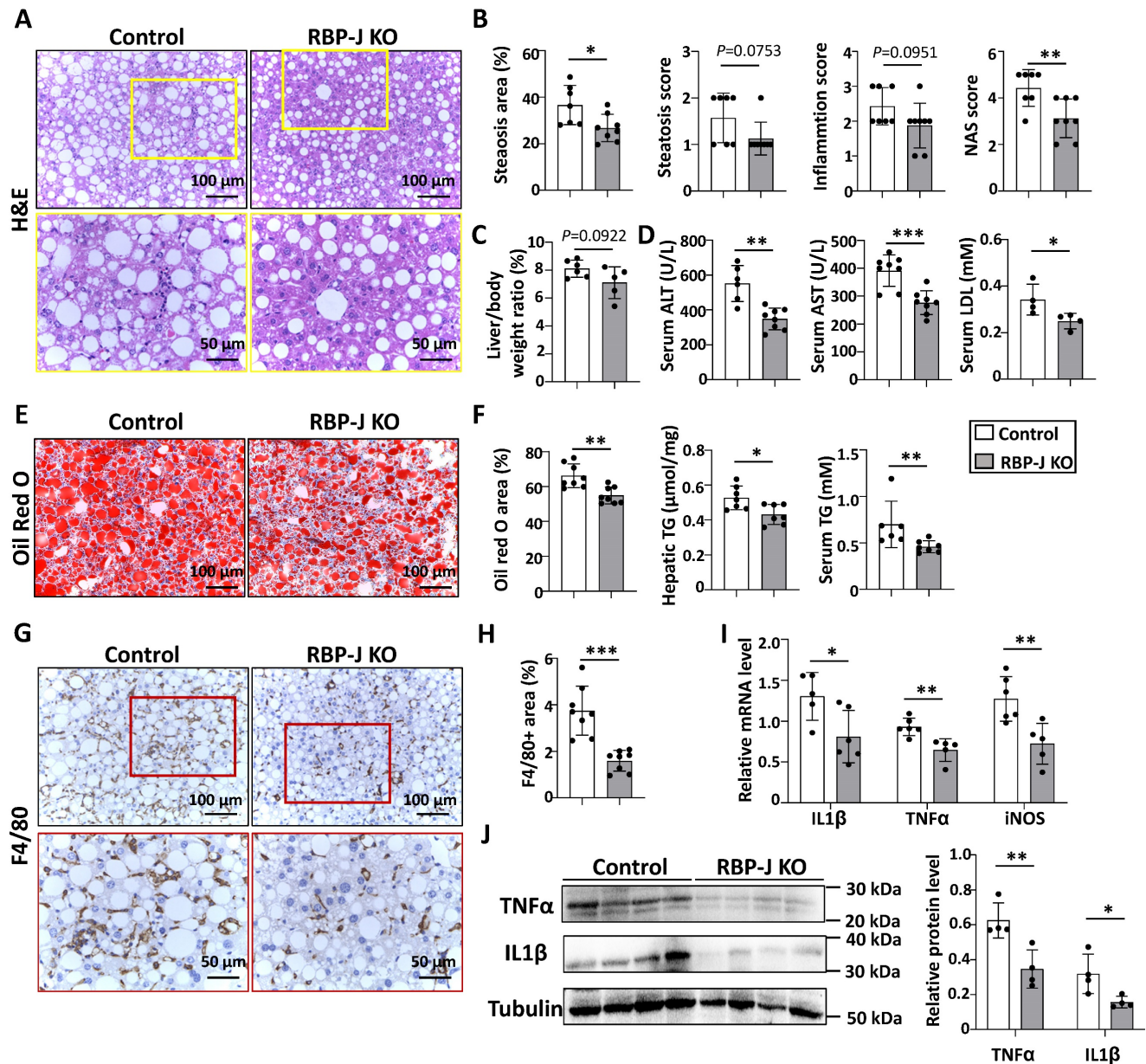


Figure 2. Myeloid-specific RBP-J deficiency attenuated experimental steatohepatitis in CDAA-fed mice. Ly2z-Cre⁺ RBP-J^{fl^{ox}/+} (Control) or Ly2z-Cre⁺ RBP-J^{fl^{ox}/fl^{ox}} (KO) mice were fed with CDAA diet for 10 weeks. (A) Liver sections were stained by H&E staining. The lower row of micrographs were a higher magnification of the yellow frames in the upper row. (B) Quantitative comparison of steatosis areas, and histological scores about steatosis, inflammation and NAS in (A). (C) Liver-to-body weight ratio. (D) Detection of ALT, AST and LDL in serum. (E) Liver sections were stained with Oil Red O. (F) Quantitative comparison of positive signals for Oil Red O in (E), and detection of triglyceride content in livers and serum. (G) Liver sections were subjected to immunohistochemical staining for F4/80. The lower row of micrographs were a higher magnification of the red frames in the upper row. (H) The positive areas of F4/80 staining in (G) were quantitatively compared. (I) The mRNA levels of IL1 β , TNF α and iNOS in livers were determined by qRT-PCR. (J) The protein levels of IL1 β and TNF α were determined by Western blot, with Tubulin as a reference control. Bars = means \pm SD; * P < 0.05, ** P < 0.01, *** P < 0.001.

The serum ALT, AST and LDL were significantly decreased compared with control mice (Fig. 2D), suggesting ameliorated liver damage in myeloid-specific RBP-J KO mice. Hematoxylin and eosin (H&E) staining showed fewer large round non-staining areas (represent lipid droplets in hepatocytes) and inflammatory cells, and lower NAS score in livers from RBP-J KO mice compared with control mice (Fig. 2A,2B). Oil red O staining of liver sections showed that RBP-J KO group had less lipid droplets compared

with control group (Fig. 2E,2F). In keeping with this, triglyceride content in serum or liver was significantly decreased in RBP-J KO mice as compared with the control mice (Fig. 2F).

Immunostaining with anti-F4/80 and anti-MPO showed that the infiltration of macrophages and neutrophils was less in livers from RBP-J KO mice (Fig. 2G,2H, Fig. S2). Accordingly, the levels of inflammatory mediators were determined using qRT-PCR and Western blot. The results indicated that

IL1 β , TNF α and iNOS were decreased in the livers from RBP-J KO mice (Figure 2I,2J). The level of IL1 β in the serum also decreased in RBP-J KO mice as compared with the control mice (Fig. S3A).

Furthermore, we evaluated hepatic fibrosis by anti-Collagen Type I Alpha 1 Chain (Col1 α 1), anti-Actin Alpha 2, Smooth Muscle (α SMA) immunostaining and Sirius red staining. RBP-J KO mice displayed significantly reduced extracellular matrix (ECM) deposition and activation of hepatic stellate cells (Fig. S4A,S4B). Consistently, the mRNA levels of tissue inhibitor of metalloproteinases 1/2 (TIMP1/2), Col1 α 1 and α SMA decreased in the livers of CDAA-fed RBP-J KO mice, while the mRNA level of matrix metalloproteinase 9 (MMP9) increased (Fig. S4C). These results indicated that RBP-J deficiency in macrophages ameliorated steatohepatitis and steatohepatitis-induced fibrosis in mice.

Notch blockade impaired the expression of IL1 β and TNF α in macrophages, and then attenuated lipid accumulation in hepatocytes *in vitro*

Next, we explored the possible mechanism of Notch blockade in macrophages affecting lipid metabolism in hepatocytes. The pro-inflammatory cytokines IL1 β and TNF α can increase lipid accumulation in hepatocytes [12, 24-26]. Meanwhile, our previous studies found that Notch blockade significantly reduced the expression of IL1 β and TNF α in macrophages [19]. Therefore, we speculate that Notch-IL1 β /TNF α axis could play a critical role during the activation of macrophages and lipid accumulation in hepatocytes.

RAW264.7 macrophages were treated with γ -secretase inhibitor DAPT, an inhibitor for Notch signaling, for 3 days. The mRNA levels of Notch target genes Hes1 and Hey1 decreased (Fig. 3B), suggesting that Notch signaling was inhibited successfully. Meanwhile, the expression of IL1 β and TNF α were determined at the mRNA and protein levels by using qRT-PCR and ELISA, respectively (Fig. 3B,3C). The results showed that the production of these inflammatory cytokines decreased significantly in DAPT-treated RAW264.7 as compared with the control. Then AML12 hepatocytes were cultured in palmitic acid medium (PA) with conditioned medium (CM) collected from each of the cultures of RAW264.7 for 2 days. We evaluated the lipid accumulation in AML12 hepatocytes by oil red O staining and triglyceride content assay. As shown in Fig. 3D-F, CM derived from DAPT-treated RAW264.7 showed reduced capacity of inducing lipid accumulation in AML12 hepatocytes, but this capacity was rescued partially by supplementing IL1 β or

TNF α , and recovered completely by supplementing IL1 β and TNF α . Meanwhile, AML12 hepatocytes were also cultured with CM derived from hepatic macrophages. As shown in Fig. S5, CM derived from RBP-J KO macrophages reduced lipid accumulation in AML12 hepatocytes, but this capacity was rescued by supplementing IL1 β or/and TNF α . Collectively, these results suggested that Notch blockade in macrophages inhibited the secretion of pro-inflammatory cytokines IL1 β and TNF α , and then ameliorated lipid accumulation in hepatocytes.

Myeloid-specific RBP-J deficiency up-regulated the expression of genes related to fatty acid degradation and peroxisomal fatty acid oxidation in livers of CDAA-fed mice

To explain how pro-inflammatory cytokines IL1 β and TNF α affect lipid accumulation in hepatocytes, we compared mRNA profiles of liver tissues between CDAA-fed RBP-J KO and control mice by using RNA-seq (Fig. S6A). Gene set enrichment analyses showed that fatty acid degradation, peroxisome, fatty acid metabolism and peroxisome proliferator activated receptor (Ppar) signaling pathway associated genes were up-regulated in RBP-J KO group (Fig. S6B). Several genes associated fatty acid metabolism, including Ppara, cytochrome P450 family 4 subfamily a member 12a (Cyp4a12a), Cyp4a12b, acetyl-CoA acyltransferase 1a (Acaa1a), nudix hydrolase 7 (Nudt7) and peroxisomal biogenesis factor 11 alpha (Pex11a), attracted our attention. As confirmed by qRT-PCR, the expression of Ppara, Cyp4a12a, Cyp4a12b, Acaa1a, Nudt7 and Pex11a were up-regulated in RBP-J KO group (Fig. S6C). Studies have shown that Cyp4a12a/b is associated with fatty acid degradation [27,28], and Acaa1a, Nudt7, Pex11a are related to peroxisomal fatty acid oxidation [29-34]. Ppara could regulate the expression of Cyp4a12a/b, Acaa1a and Pex11a [27-30,34]. Knockout of Acaa1a, Nudt7 or Pex11a promoted hepatic steatosis [30-33]. Meanwhile, hepatic macrophages promoted hepatic steatosis via IL1 β -dependent suppression of Ppara activity [24]. Loft et al. also found that TNF α expressed by macrophages could affect the activity of Ppara in hepatocytes and inhibit the expression of Ppara downstream genes [35]. Therefore, we speculated that RBP-J knockout in macrophages reduced the expression of IL1 β and TNF α , and these reduced inflammatory factors could increase the expression or activity of Ppara in hepatocytes and then up-regulate the expression of genes related to fatty acid degradation and peroxisomal fatty acid oxidation, which ultimately would reduce fat accumulation.

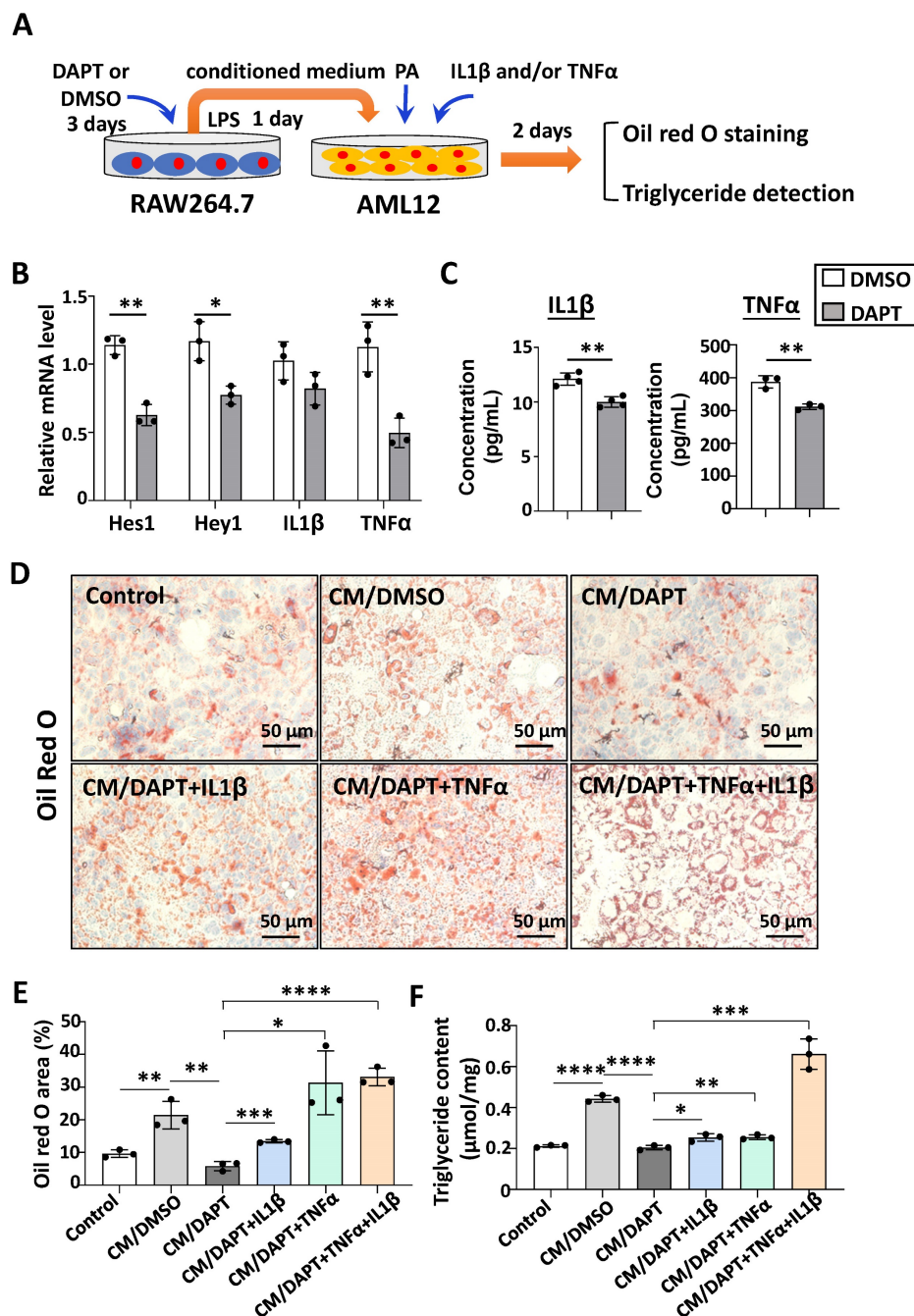


Figure 3. Notch blockade in macrophages attenuated lipid accumulation in hepatocytes through inhibiting the expression of IL1β and TNFα *in vitro*. (A) Schematic showing that RAW264.7 macrophages were treated with γ -secretase inhibitor DAPT (5 μ M) for 3 days, changed and cultured with the fresh medium containing LPS (100 ng/ml) for 1 day, and the conditioned medium (CM) were harvested. Then AML12 hepatocytes were cultured with CM, in the presence or absence of TNFα (10 ng/ml), and/or IL1β (10 ng/ml) in palmitic acid medium (PA, 10 mM) for 2 days. (B) The mRNA levels of Hes1, Hey1, IL1β and TNFα in RAW264.7 macrophages treated with DMSO or DAPT were determined by qRT-PCR. (C) The levels of IL1β and TNFα in RAW264.7 culture supernatants were measured by ELISA. (D) Lipid accumulation in AML12 cells was assessed with Oil Red O staining. (E) The positive areas of Oil Red O staining in (D) were quantitatively compared. (F) Triglyceride content in AML12 hepatocytes was measured. Bars = means \pm SD; * $P < 0.05$, ** $P < 0.01$, *** $P < 0.001$, **** $P < 0.0001$.

Characterization of exosomes derived from bEnd.3 cells

We examined the effects of Notch inhibition in macrophages on the development of steatohepatitis. In our previous work, we demonstrated that exosomes loaded with RBP-J decoy could inhibit Notch signaling in hepatic macrophages and ameliorate

CCl₄- or BDL-induced liver fibrosis in mice [20]. It is natural to ask whether this therapeutic strategy can be extended to steatohepatitis.

Exosomes isolated from culture supernatants of a mouse endothelial cell line bEnd.3 to further reduce the immunogenicity of exosomes compared with HEK293T. As determined by Western blot, bEnd.3-derived exosomes had an enrichment of exosomal

marker proteins CD9 and Alix, and contained a small amount of flotillin-1, whereas the expression of mitochondrial membrane protein VDAC1 was undetectable (Fig. 4A). NTA assay showed that the particle size of most bEnd.3-derived exosomes was below 200 nm, and electroporation had no significant effect on its particle size (Fig. 4B). Moreover, TEM indicated that the exosomes had a bilayer structure and electroporation has little effect on its morphology (Fig. 4C).

Exosomes delivered via the tail vein were mainly taken up by hepatic macrophages and inhibited macrophage Notch signaling in a murine model of steatohepatitis

We tested the distribution of exosomes injected intravenously in steatohepatitis. We established a mouse model of steatohepatitis by feeding CDAA diet. Mice were infused with DiI-labeled exosomes (200 $\mu\text{g}/\text{mouse}$) via the tail vein. As expected, bioluminescence imaging analysis showed that DiI-labeled exosomes were mainly distributed in the liver 6 h after injection (Fig. 4D). Moreover,

immunofluorescence staining of liver sections indicated DiI-labeled exosomes mainly located in F4/80⁺ macrophages 6 h after injection (Fig. 4E). These findings suggested that bEnd.3-derived exosomes were taken up by hepatic macrophages in mice with steatohepatitis.

We next assessed if exosomes loaded with RBP-J ODNs were functional in hepatic macrophages. ODNs were loaded into bEnd.3-derived exosomes by electroporation, as previously reported [20, 23]. CDAA-fed mice were injected with Exo-RBP-J decoy or Exo-control decoy ODNs via the tail vein (Fig. 5A). Hepatic F4/80⁺ cells were isolated using MACS as previously reported [20]. As determined by qRT-PCR, the levels of Hes1, Hey1, IL1 β and TNF α were downregulated in hepatic F4/80⁺ cells derived from Exo-RBP-J decoy ODN-treated mice compared with mice treated with Exo-control decoy ODNs (Fig. 4F). These results suggested that exosomes loaded with RBP-J decoy ODNs could inhibit the activation of Notch signaling in hepatic macrophages *in vivo*.

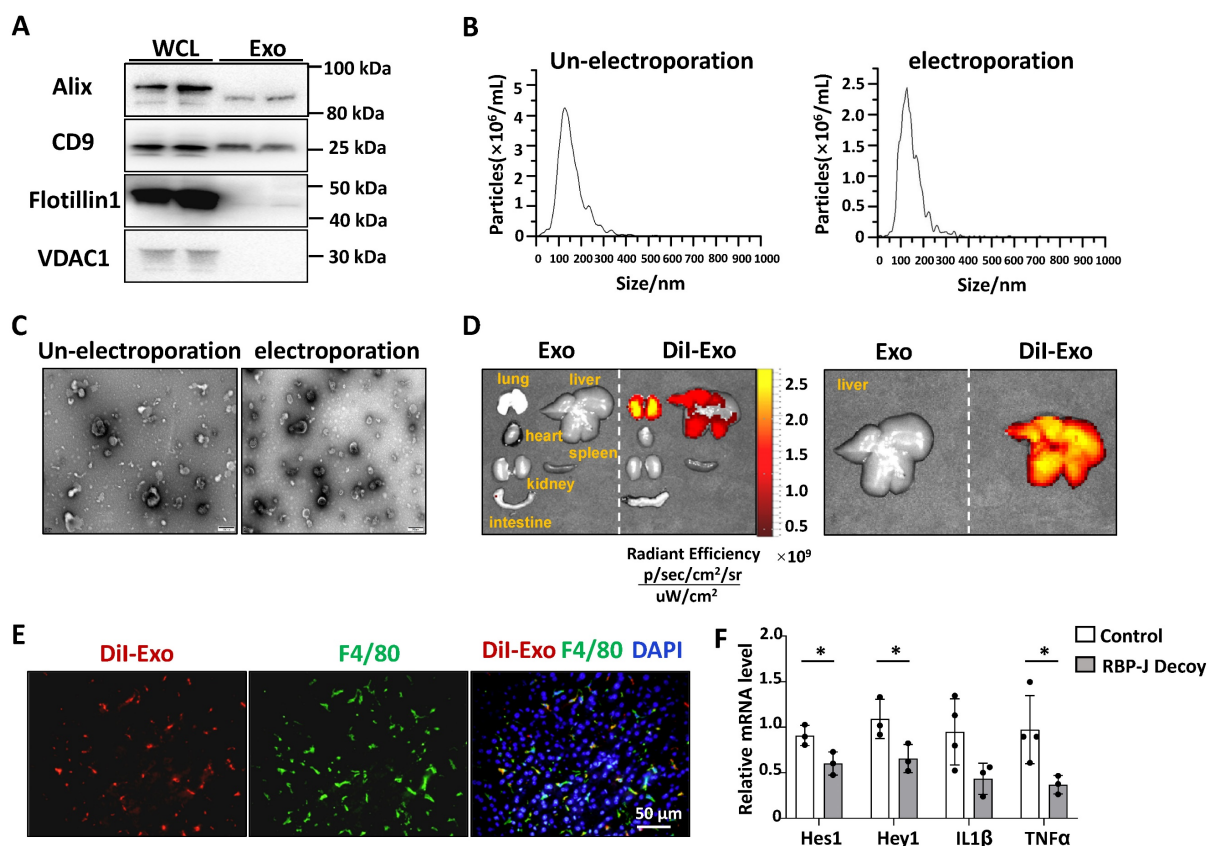


Figure 4. Exosomes loaded with RBP-J decoy oligodeoxynucleotide (ODNs) inhibited Notch signaling in hepatic macrophages in a murine model of steatohepatitis. (A-C) Characterization of exosomes derived from bEnd.3 cells. (A) The levels of CD9, Alix, flotillin-1, and VDAC1 in exosomes and bEnd.3 cells lysates were determined by western blot. (B) The size distribution of exosomes was determined by nanoparticle tracking analysis (NTA). (C) Exosome morphology was observed by transmission electron microscopy (TEM). (D) Exosomes were stained with DiI and approximately 200 μg (protein equivalent) of exosomes in 150 μL of PBS were injected via the tail vein into mice with CDAA-induced steatohepatitis. After 6 h, DiI signals in the liver, lung, spleen, intestine, kidney, and heart were examined using bioluminescence imaging. (E) 6 h after injection of DiI-labeled exosomes, liver sections were stained with an anti-mouse F4/80 antibody and analyzed by fluorescence microscopy. Nuclei were counterstained with DAPI. (F) Mice were fed with CDAA diet for 10 weeks, and exosomes loaded with RBP-J decoy or control decoy ODNs (exosomes/decoy ODNs = 200 $\mu\text{g}/2.5$ nmol) were injected into mice four times via tail vein at the last 2 weeks. F4/80⁺ hepatic macrophages were isolated using magnetic-activated cell sorting (MACS). The mRNA levels of Hes1, Hey1, TNF α , and IL1 β in F4/80⁺ hepatic macrophages were measured by qRT-PCR. Bars = means \pm SD; * P < 0.05.

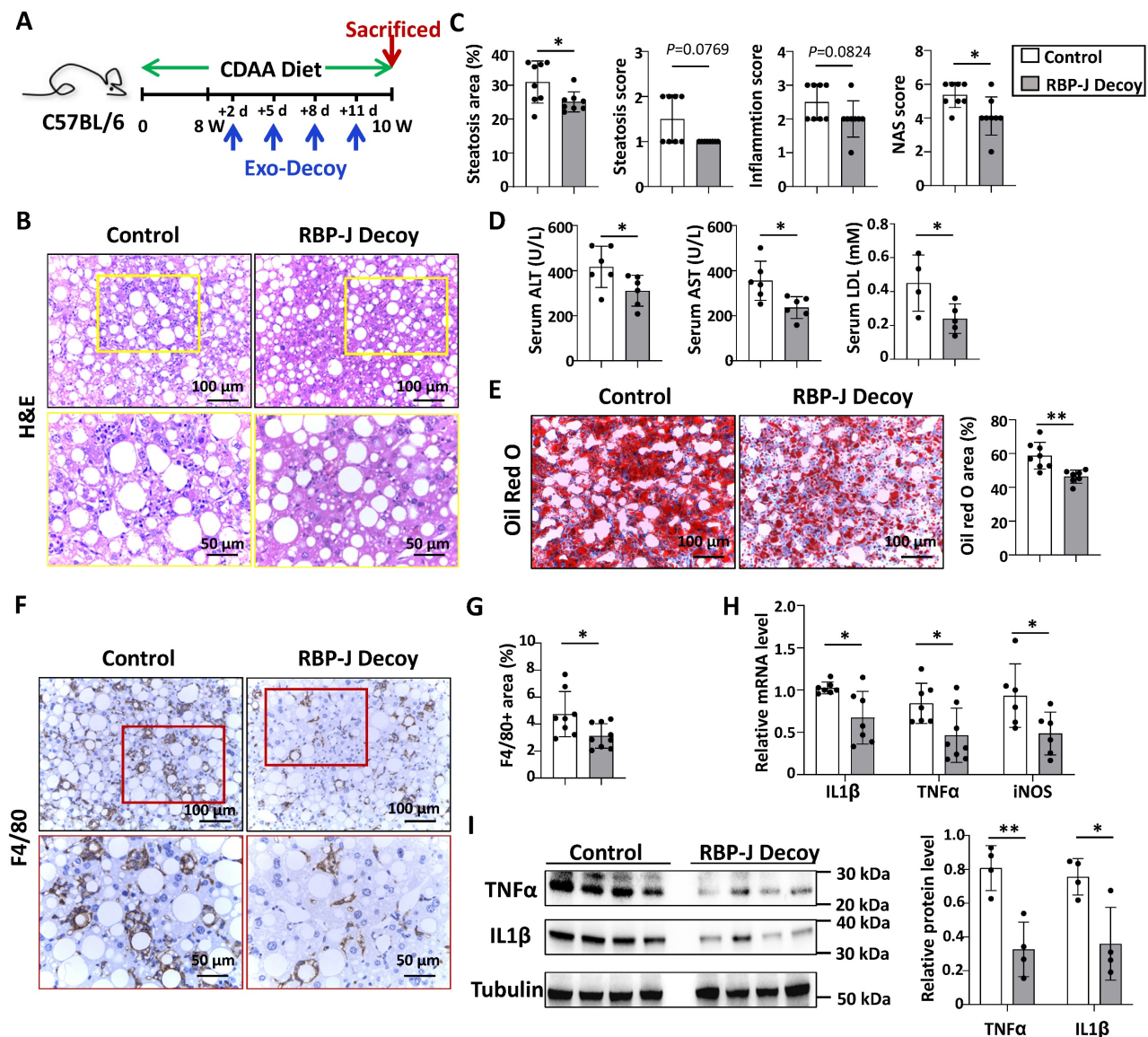


Figure 5. Exosomes loaded with RBP-J decoy ODNs attenuated experimental steatohepatitis in CDAA-fed mice. (A) Schematic illustration of the procedure used for exosomes loaded with RBP-J decoy ODNs or control decoy ODNs to treat steatohepatitis in mice fed with CDAA diet. (B) Liver sections were stained by H&E staining. The lower row of micrographs were a higher magnification of the yellow frames in the upper row. (C) Quantitative comparison of steatosis areas, and histological scores about steatosis, inflammation and NAS in (B). (D) Detection of ALT, AST and LDL in serum. (E) Liver sections were stained with Oil Red O, and areas positive were quantified and compared. (F) Liver sections were subjected to immunohistochemical staining for F4/80. The lower row of micrographs were a higher magnification of the red frames in the upper row. (G) The positive areas of F4/80 staining in (F) were quantitatively compared. (H) The mRNA levels of IL1 β , TNF α and iNOS in livers were determined by qRT-PCR. (I) The protein levels of IL1 β and TNF α were determined by Western blot, with Tubulin as a reference control. Bars = means \pm SD, * P < 0.05, ** P < 0.01.

Exo-RBP-J decoy ODNs attenuated experimental steatohepatitis in CDAA-fed or steatosis in HFD-fed mice

Next, we evaluated the efficacy of Exo-RBP-J decoy ODNs in CDAA-fed or HFD-fed mice. As shown in Fig. 5A, mice were fed with CDAA diet for 10 weeks, and infused four times with Exo-RBP-J decoy or Exo-control decoy ODNs (200 μ g/mouse) via tail vein during the last 2 weeks. H&E staining of liver sections showed that the large round non-staining areas and infiltrating cells were less in Exo-RBP-J decoy ODN-treated group compared with control (Fig. 5B,5C). Meanwhile, liver sections were

assessed with NAS score. The results indicated that NAS score in Exo-RBP-J decoy ODN-treated mice were lower than control mice (Fig. 5C). Accordingly, Oil Red O staining of liver sections also showed that Exo-RBP-J decoy ODN-treated mice had less lipid accumulation in livers compared with control mice (Fig. 5E). Immunostaining with anti-F4/80 and anti-MPO showed that the infiltration of macrophages and neutrophils was less in livers from Exo-RBP-J decoy ODN-treated mice (Fig. 5F,5G, Fig. S7). Accordingly, the levels of inflammatory mediators were determined using qRT-PCR and Western blot. The results indicated that IL1 β , TNF α and iNOS were

decreased in the livers from mice treated with Exo-RBP-J decoy ODNs (Fig. 5H,I). The level of IL1 β in the serum also decreased in Exo-RBP-J decoy ODNs treated mice as compared with the control mice (Fig. S3B). In keeping with this, serum ALT, AST and LDL levels were decreased in Exo-Decoy RBP-J ODN recipient mice, suggesting that liver function had improved (Fig. 5D). Then we evaluated hepatic fibrosis by anti- α SMA, anti-Col1 α immunohistochemical staining and Sirius red staining. Exo-RBP-J decoy ODN-treated mice displayed significantly decreased activation of hepatic stellate cells and ECM deposition (Fig. S8A,B). Consistently, the mRNA levels of platelet derived growth factor subunit B (PDGF-B), TIMP2, Col1 α 1 and α SMA decreased in the livers of Exo-RBP-J decoy ODN-treated mice (Fig. S8C). These results indicated that Exo-RBP-J decoy ODNs ameliorated steatohepatitis and steatohepatitis-induced fibrosis in CDAA-fed mice.

To confirm the effect of Exo-RBP-J decoy ODNs in NAFLD, the experiment was repeated using another mouse model, HFD-induced steatosis. As shown in Fig 6A, mice were fed with HFD diet for 22 weeks, and infused four times with Exo-RBP-J decoy or Exo-control decoy ODNs via tail vein during the last 2 weeks. Histological examination of liver sections

using with H&E or oil red O staining showed that Exo-RBP-J decoy ODNs-treated mice had less lipid accumulation in livers compared with control mice (Fig. 6B,C,E,F). Meanwhile, NAS score was also decreased in the livers of Exo-RBP-J decoy ODN-treated mice (Fig. 6C). Accordingly, triglyceride content and LDL in serum were significantly decreased in Exo-RBP-J decoy ODNs-treated mice (Fig. 6D). Overall, these data suggested that Exo-RBP-J decoy ODNs application could attenuate experimental steatohepatitis in CDAA-fed or steatosis in HFD-fed mice.

Discussion

Studies have shown that Notch signaling can regulate key processes of in liver development, homeostasis, and disease [36-38]. Pajvani's group demonstrated that hepatocyte Notch signaling was activated in patients with NASH and a mouse model of diet-induced NASH [39,40]. They further developed a poly(lactic coglycolic acid) (PLGA)-encapsulated γ -secretase inhibitor nanoparticles (GSI NPs) to target hepatocytes, and found that GSI NPs application ameliorated liver inflammation and fibrosis in NASH diet-fed mice [41].

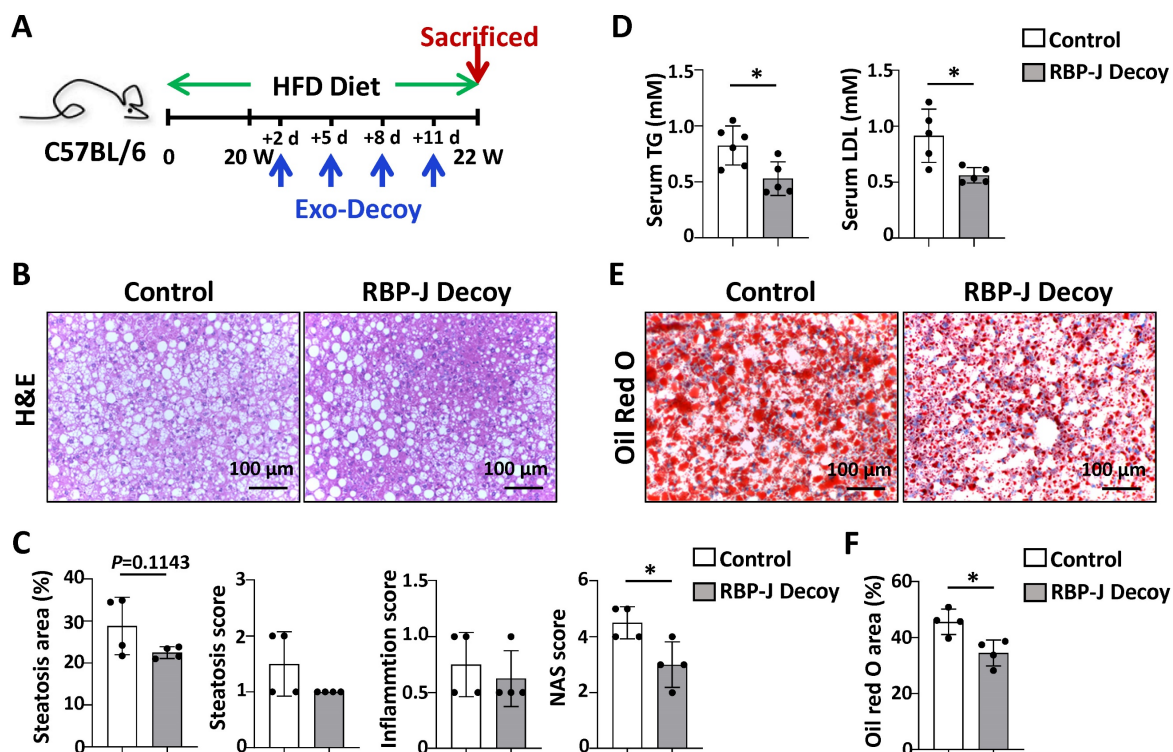


Figure 6. Exosomes loaded with RBP-J decoy ODNs attenuated fatty liver in HFD-fed mice. (A) Schematic illustration of the procedure used for exosomes loaded with RBP-J decoy ODNs or control decoy ODNs to treat steatosis in HFD diet-fed mice. Mice were fed with HFD diet for 22 weeks, and exosomes loaded with RBP-J decoy or control decoy ODNs (exosomes/decoy ODNs = 200 μ g/2.5 nmol) were injected into mice four times via tail vein at the last 2 weeks. (B) Liver sections were stained by H&E staining. (C) Quantitative comparison of steatosis areas, and histological scores about steatosis, inflammation and NAS in (B). (D) Detection of triglyceride content and LDL in serum. (E) Liver sections were stained with Oil Red O, and areas positive were quantified and compared in (F). Bars = means \pm SD; * $P < 0.05$.

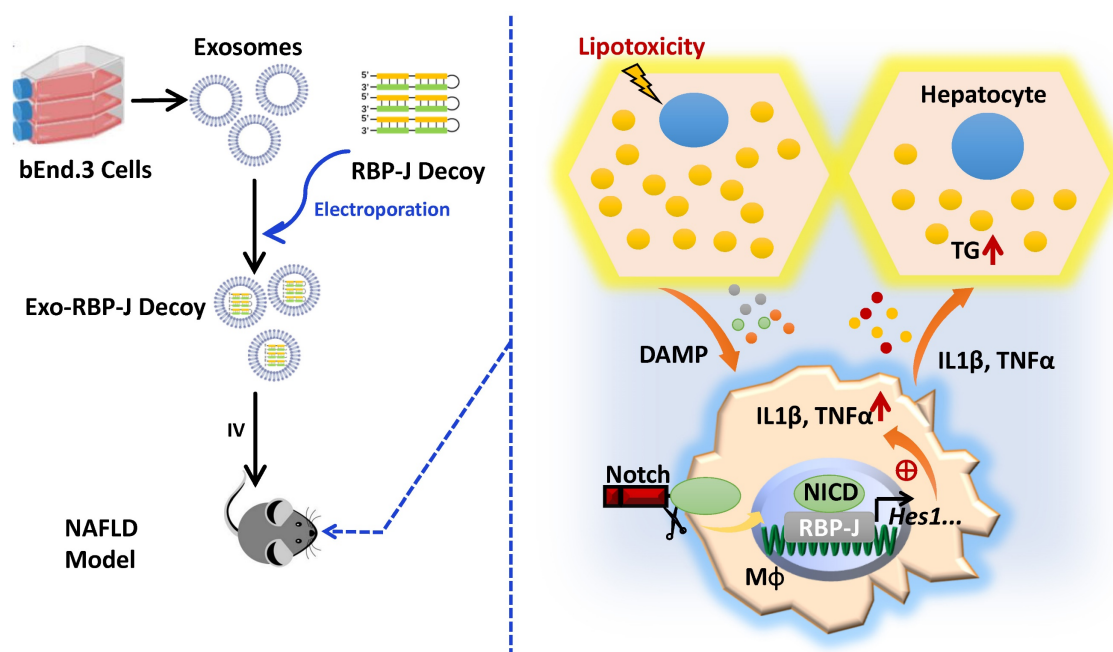


Figure 7. Schematic summary of this study. During the progression of NAFLD, injured hepatocytes caused by over-accumulated lipid toxicity, released damage-associated molecular patterns (DAMPs), and then stimulated hepatic macrophages to release pro-inflammatory cytokines such as IL1 β , TNF α . Meanwhile, Notch signaling, mediated by transcription factor RBP-J, was activated in hepatic macrophages and further promoted the expression of IL1 β and TNF α . And then IL1 β and TNF α in turn enhanced lipid accumulation in hepatocytes. Next, we used exosomes targeting delivery of RBP-J decoy ODNs and inhibited the activation of Notch signaling in macrophages. Finally, the infused exosomes-RBP-J decoy ODNs via tail vein resulted in the amelioration of NAFLD in mice.

Interestingly, in this study we found that Notch signaling was activated in hepatic macrophages in human with NASH or in CDAA-fed mice. Several groups have reported that Notch signaling regulates macrophage activation through multiple downstream molecules, such as IRF8, SOCS3, Cyld, miR-125a, miR-148a and signal regulatory protein α (SIRP α) [15-19,42-44]. Therefore, we speculated that macrophage Notch signaling may play a role in the development of NAFLD. We then established a CDAA-induced steatohepatitis model in *Lyz2-Cre RBP-J^{fllox}* mice and found that myeloid-specific RBP-J deficiency attenuated liver inflammation, lipid accumulation and hepatic fibrosis. Similar to our previous results in *CCL₄*-induced hepatic fibrosis, the expression of inflammatory factors IL1 β and TNF α was significantly decreased in the livers of myeloid-specific RBP-J knockout mice with NAFLD in this study. As we known, macrophage-derived inflammatory mediators may influence hepatocyte steatosis. Stienstra et al. [24] reported that hepatic macrophages promoted hepatic steatosis via IL1 β -dependent suppression of Ppara activity. Miura et al. [25] showed that IL1 β derived from hepatic macrophages increased lipid accumulation in hepatocytes. Zhang et al. [12] reported that macrophage p38a could promote lipid accumulation in hepatocytes through the induction of cytokines TNF α , CXCL10 and IL6. Diehl et al. [26] also showed that TNF α secretion by hepatic macrophages was necessary and

sufficient to induce steatosis in hepatocytes *in vitro*. And our results indicated that CM derived from macrophages treated with GSI reduced lipid accumulation in hepatocytes, but this capacity was rescued partially by supplement of IL1 β or TNF α , and recovered completely by supplement of IL1 β and TNF α .

To explain how pro-inflammatory cytokines IL1 β and TNF α affect lipid accumulation in hepatocytes, we examined the expression of classical genes associated with fatty acid metabolism in the liver samples of CDAA-fed RBP-J KO and control mice. However, we didn't obtain differentially expressed genes except *Ppara*. Therefore, we compared mRNA profiles of liver tissues between CDAA-fed RBP-J KO and control mice by using RNA-seq. We found that the expression of *Ppara*, *Cyp4a12a/b*, *Acaa1a*, *Nudt7* and *Pex11a* was up-regulated in RBP-J knockout group. Interestingly, these genes, which are regulated by *Ppara*, are closely related to peroxisomal fatty acid oxidation and fatty acid degradation [27-34]. Naturally, we speculated that macrophage RBP-J knockout can attenuate the expression of TNF α and IL1 β , then the reduced TNF α and IL1 β may enhance the expression or activity of *Ppara* in hepatocytes, up-regulate the expression of *Cyp4a12a/b*, *Acaa1a* and *Pex11a*, promote peroxisomal fatty acids oxidation and fatty acid degradation, and finally reduce lipid accumulation in hepatocytes. This hypothesis deserves further study.

We then sought to determine the feasibility of treating NAFLD by inhibiting Notch signaling in macrophages. Several key points need to be weighed carefully. First, selecting a proper drug delivery system to target hepatic macrophages. Exosomes are nano-sized phospholipid bilayer-enclosed vesicles secreted by living cells and have the advantage of lower immunogenicity compared with exogenous nanocarriers [45, 46]. Importantly, exosomes injected intravenously were mainly distributed in the liver and taken up by hepatic macrophages [47, 48]. This indicates that exosomes may represent a natural delivery system for the targeting of hepatic macrophages. In this study, we further demonstrated that exosomes injected via tail vein were taken up by hepatic macrophages in CDAA-fed mice.

Second, selecting appropriate Notch inhibitor. Transcription factor decoy (TFD) ODNs harboring the consensus DNA recognition motif of a target transcription factor can compete with the binding sites in the promoter regions of target genes for the binding of transcription factor, and significantly reduce the expression levels of downstream genes [49]. Several studies have investigated the application of NF- κ B decoy ODNs in the treatment of inflammatory disorders [50,51]. We previously have systematically demonstrated that RBP-J decoy ODNs can inhibit the activation of Notch signaling in macrophages [20].

Third, we need to evaluate the efficiency for ODNs loading into exosomes. As previously reported, the efficiency of electroporation was about 9% [20]. Exosomes can also be loaded with drugs by other methods, such as co-incubation, ultrasound treatment, saponin treatment, density gradient ultracentrifugation, and freeze-thaw extrusion [52]. We will compare the drug delivery efficiency of other methods in the future work.

Finally, we need to confirm that exosomes loaded with RBP-J decoy ODNs could work after entering macrophages. Exosomes could be internalized into mammalian cells mainly by two different mechanisms including direct membrane fusion and endocytosis [53]. Parolini et al. [54] and Montecalvo et al. [55]. verified that the cargoes would release to the cytosol once exosomes have fused with membrane. On the other hand, exosomes enter cells through the endocytosis pathway [53]. To complete cargo delivery, exosomes need to escape the endo/lysosomal membrane, a process is known as "endosomal escape". Although there is currently no direct evidence that exosomes can escape the endo/lysosome, numerous studies have claimed that exosomes can functionally deliver cargo to recipient cells and induce substantial phenotypic changes

[56-60]. As for our study, we sorted hepatic macrophages from CDAA mice, detected the expression of Notch downstream genes, and functionally verified the inhibitory effects of RBP-J decoy ODNs *in vivo*.

Studies have shown that hepatic macrophages are a heterogeneous population of immune cells, consisted of resident macrophages (Kupffer cells) and monocyte-derived macrophages. Kupffer cells are established during embryonic development from fetal yolk-sack, whereas monocyte-derived macrophages originate from circulating monocytes [6-8]. The RBP-J gene of Kupffer cells or monocyte-derived macrophages was deficient in *Lyz2-Cre RBP-J^{flox/flox}* transgenic mice (data not shown). What are the effects of different macrophage populations on NAFLD? Does Notch signaling play a role among them? This deserves further study.

In summary, we demonstrated that Notch signaling was activated in hepatic macrophages in human with NASH or in mice with experimental steatohepatitis. We found that myeloid-specific RBP-J deficiency could attenuate experimental steatohepatitis in mice. One of the mechanisms may be that Notch signaling blockade attenuates the expression of inflammatory cytokines IL1 β and TNF α in macrophages, thereby inhibits lipid accumulation in hepatocytes by enhancing peroxisomal fatty acid oxidation. Furthermore, our results showed that injection of exosomes loaded with RBP-J decoy ODNs via tail vein could efficiently inhibit Notch signaling in hepatic macrophages, and ameliorate NAFLD in mice. Thus, infusion of exosomes loaded with RBP-J decoy ODNs may represent a promising therapeutic strategy for the treatment of NAFLD that merits further investigation.

Supplementary Material

Supplementary figures and tables.

<https://www.ijbs.com/v19p1941s1.pdf>

Acknowledgments

We would like to give special thanks to Professor Han for the gift of *Lyz2-Cre RBP-J^{flox}* transgenic mice.

Funding

This work was supported by grants from the National Key Research and Development Program of China (2021YFA1100500, 2016YFA0102100) and National Natural Science Foundation of China (Grant No. 81970535, 81422009, 81770560).

Ethical Approval

All animal procedures used in this study were approved by the Ethics Committee of Fourth Military Medical University.

Statement of Human and Animal Rights

All procedures in this study were conducted in accordance with the approved protocols of the Ethics Committee of Fourth Military Medical University.

Statement of Informed Consent

All procedures were approved by the Human Ethics Committees of Xijing Hospital. All participants provided informed written consent.

Competing Interests

The authors have declared that no competing interest exists.

References

1. Younossi ZM, Koenig AB, Abdelatif D, Fazel Y, Henry L, Wymer M. Global epidemiology of nonalcoholic fatty liver disease-Meta-analytic assessment of prevalence, incidence, and outcomes. *Hepatology*. 2016;64:73-84.
2. Diehl AM, Day C. Cause, Pathogenesis, and Treatment of Nonalcoholic Steatohepatitis. *N Engl J Med*. 2017;377:2063-2072.
3. Powell EE, Wong VW, Rinella M. Non-alcoholic fatty liver disease. *Lancet*. 2021;397:2212-2224.
4. Heymann F, Tacke F. Immunology in the liver—from homeostasis to disease. *Nat Rev Gastroenterol Hepatol*. 2016;13:88-110.
5. Gao CC, Bai J, Han H, Qin HY. The versatility of macrophage heterogeneity in liver fibrosis. *Front Immunol*. 2022;13:968879.
6. Cha JY, Kim DH, Chun KH. The role of hepatic macrophages in nonalcoholic fatty liver disease and nonalcoholic steatohepatitis. *Lab Anim Res*. 2018;34:133-139.
7. Kazankov K, Jørgensen SMD, Thomsen KL, Møller HJ, Vilstrup H, George J, et al. The role of macrophages in nonalcoholic fatty liver disease and nonalcoholic steatohepatitis. *Nat Rev Gastroenterol Hepatol*. 2019;16:145-159.
8. Wen Y, Lambrecht J, Ju C, Tacke F. Hepatic macrophages in liver homeostasis and diseases-diversity, plasticity and therapeutic opportunities. *Cell Mol Immunol*. 2021;18:45-56.
9. Murray PJ, Wynn TA. Protective and pathogenic functions of macrophage subsets. *Nat Rev Immunol*. 2011;11:723-37.
10. Wang C, Ma C, Gong L, Guo Y, Fu K, Zhang Y, et al. Macrophage Polarization and Its Role in Liver Disease. *Front Immunol*. 2021;12:803037.
11. Wan J, Benkdane M, Teixeira-Clerc F, Bonnafous S, Louvet A, Lafdil F, et al. M2 Kupffer cells promote M1 Kupffer cell apoptosis: a protective mechanism against alcoholic and nonalcoholic fatty liver disease. *Hepatology*. 2014;59:130-42.
12. Zhang X, Fan L, Wu J, Xu H, Leung WY, Fu K, et al. Macrophage p38 α promotes nutritional steatohepatitis through M1 polarization. *J Hepatol*. 2019;71:163-174.
13. Odegaard JL, Ricardo-Gonzalez RR, Red Eagle A, Vats D, Morel CR, Goforth MH, et al. Alternative M2 activation of Kupffer cells by PPAR δ ameliorates obesity-induced insulin resistance. *Cell Metab*. 2008;7:496-507.
14. Artavanis-Tsakonas S, Rand MD, Lake RJ. Notch signaling: cell fate control and signal integration in development. *Science*. 1999;284:770-6.
15. Wang YC, He F, Feng F, Liu XW, Dong GY, Qin HY, et al. Notch signaling determines the M1 versus M2 polarization of macrophages in antitumor immune responses. *Cancer Res* 2010;70:4840-49.
16. Zhang W, Xu W, Xiong S. Blockade of Notch1 signaling alleviates murine lupus via blunting macrophage activation and M2b polarization. *J Immunol*. 2010;184:6465-78.
17. Xu H, Zhu J, Smith S, Foldi J, Zhao B, Chung AY, et al. Notch-RBP-J signaling regulates the transcription factor IRF8 to promote inflammatory macrophage polarization. *Nat Immunol*. 2012;13:642-50.
18. Monsalve E, Ruiz-García A, Baladrón V, Ruiz-Hidalgo MJ, Sánchez-Solana B, Rivero S, et al. Notch1 upregulates LPS-induced macrophage activation by increasing NF- κ B activity. *Eur J Immunol*. 2009;39:2556-70.
19. He F, Guo FC, Li Z, Yu HC, Ma PF, Zhao JL, et al. Myeloid-specific disruption of recombination signal binding protein j κ ameliorates hepatic fibrosis by attenuating inflammation through cylindromatosis in mice. *Hepatology*. 2015;61:303-14.
20. He F, Li WN, Li XX, Yue KY, Duan JL, Ruan B, et al. Exosome-mediated delivery of RBP-J decoy oligodeoxynucleotides ameliorates hepatic fibrosis in mice. *Theranostics*. 2022;12:1816-28.
21. Yue KY, Zhang PR, Zheng MH, Cao XL, Cao Y, Zhang YZ, et al. Neurons can upregulate Cav-1 to increase intake of endothelial cells-derived extracellular vesicles that attenuate apoptosis via miR-1290. *Cell Death Dis*. 2019;10:869.
22. Tun T, Hamaguchi Y, Matsunami N, Furukawa T, Honjo T, Kawaichi M. Recognition sequence of a highly conserved DNA binding protein RBP-J κ . *Nucleic Acids Res*. 1994;22:965-71.
23. Alvarez-Erviti L, Seow Y, Yin H, Betts C, Lakkal S, Wood MJ. Delivery of siRNA to the mouse brain by systemic injection of targeted exosomes. *Nat Biotechnol*. 2011;29:341-5.
24. Stienstra R, Saudale F, Duval C, Keshtkar S, Groener JE, van Rooijen N, et al. Kupffer cells promote hepatic steatosis via interleukin-1 β -dependent suppression of peroxisome proliferator-activated receptor α activity. *Hepatology*. 2010;51:511-22.
25. Miura K, Kodama Y, Inokuchi S, Schnabl B, Aoyama T, Ohnishi H, et al. Toll-like receptor 9 promotes steatohepatitis by induction of interleukin-1 β in mice. *Gastroenterology*. 2010;139:323-34.
26. Diehl KL, Vorac J, Hofmann K, Meiser P, Unterwiesing I, Kuerschner L, et al. Kupffer Cells Sense Free Fatty Acids and Regulate Hepatic Lipid Metabolism in High-Fat Diet and Inflammation. *Cells*. 2020;9:2258.
27. Jeffery B, Choudhury AI, Horley N, Bruce M, Tomlinson SR, Roberts RA, et al. Peroxisome proliferator activated receptor α regulates a male-specific cytochrome P450 in mouse liver. *Arch Biochem Biophys*. 2004;429:231-6.
28. Le Bouquin R, Lugnier A, Frossard N, Pons F. Expression of cytochrome P450 4A mRNA in mouse lung: effect of clofibrate and interleukin-1 β . *Fundam Clin Pharmacol*. 2004;18:181-6.
29. Lee SS, Pineau T, Drago J, Lee EJ, Owens JW, Kroetz DL, et al. Targeted disruption of the α isoform of the peroxisome proliferator-activated receptor gene in mice results in abolishment of the pleiotropic effects of peroxisome proliferators. *Mol Cell Biol*. 1995;15:3012-22.
30. Arnaud S, Fidaleo M, Clémencet MC, Chevillard G, Athias A, Gresti J, et al. Modulation of the hepatic fatty acid pool in peroxisomal 3-ketoacyl-CoA thiolase B-null mice exposed to the selective PPAR α agonist Wy14,643. *Biochimie*. 2009;91:1376-86.
31. Song J, Baek IJ, Park S, Oh J, Kim D, Song K, et al. Deficiency of peroxisomal NUDT7 stimulates *de novo* lipogenesis in hepatocytes. *iScience*. 2022;25:105135.
32. Chen C, Wang H, Chen B, Chen D, Lu C, Li H, et al. Pex11a deficiency causes dyslipidaemia and obesity in mice. *J Cell Mol Med*. 2019;23:2020-31.
33. Weng H, Ji X, Naito Y, Endo K, Ma X, Takahashi R, et al. Pex11 α deficiency impairs peroxisome elongation and division and contributes to nonalcoholic fatty liver in mice. *Am J Physiol Endocrinol Metab*. 2013;304:E187-96.
34. Shimizu M, Takeshita A, Tsukamoto T, Gonzalez FJ, Osumi T. Tissue-selective, bidirectional regulation of PEX11 α and perilipin genes through a common peroxisome proliferator response element. *Mol Cell Biol*. 2004;24:1313-23.
35. Loft A, Schmidt SF, Caratti G, Stifel U, Havelund J, Sekar R, et al. A macrophage-hepatocyte glucocorticoid receptor axis coordinates fasting ketogenesis. *Cell Metab*. 2022;34:473-86.
36. Morell CM, Strazzabosco M. Notch signaling and new therapeutic options in liver disease. *J Hepatol*. 2014;60:885-90.
37. Geisler F, Strazzabosco M. Emerging roles of Notch signaling in liver disease. *Hepatology*. 2015;61:382-92.
38. Xu H, Wang L. The Role of Notch Signaling Pathway in Non-Alcoholic Fatty Liver Disease. *Front Mol Biosci*. 2021;8:792667.
39. Zhu C, Kim K, Wang X, Bartolome A, Salomao M, Dongiovanni P, et al. Hepatocyte Notch activation induces liver fibrosis in nonalcoholic steatohepatitis. *Sci Transl Med*. 2018;10:eaat0344.
40. Yu J, Zhu C, Wang X, Kim K, Bartolome A, Dongiovanni P, et al. Hepatocyte TLR4 triggers inter-hepatocyte Jagged1/Notch signaling to determine NASH-induced fibrosis. *Sci Transl Med*. 2021;13:eabe1692.
41. Richter LR, Wan Q, Wen D, Zhang Y, Yu J, Kang JK, et al. Targeted Delivery of Notch Inhibitor Attenuates Obesity-Induced Glucose Intolerance and Liver Fibrosis. *ACS Nano*. 2020;14:6878-6886.
42. Huang F, Zhao JL, Wang L, Gao CC, Liang SQ, An DJ, et al. miR-148a-3p Mediates Notch Signaling to Promote the Differentiation and M1 Activation of Macrophages. *Front Immunol*. 2017;8:1327.
43. Zhao JL, Huang F, He F, Gao CC, Liang SQ, Ma PF, et al. Forced Activation of Notch in Macrophages Represses Tumor Growth by Upregulating miR-125a and Disabling Tumor-Associated Macrophages. *Cancer Res*. 2016;76:1403-15.
44. Lin Y, Zhao JL, Zheng QJ, Jiang X, Tian J, Liang SQ, et al. Notch Signaling Modulates Macrophage Polarization and Phagocytosis Through Direct Suppression of Signal Regulatory Protein α Expression. *Front Immunol*. 2018;9:1744.
45. EL Andaloussi S, Mäger I, Breakefield XO, Wood MJ. Extracellular vesicles: biology and emerging therapeutic opportunities. *Nat Rev Drug Discov*. 2013;12:347-57.
46. Valadi H, Ekström K, Bossios A, Sjöstrand M, Lee JJ, Lötvall JO. Exosome-mediated transfer of mRNAs and microRNAs is a novel mechanism of genetic exchange between cells. *Nat Cell Biol*. 2007;9:654-9.
47. Imai T, Takahashi Y, Nishikawa M, Kato K, Morishita M, Yamashita T, et al. Macrophage-dependent clearance of systemically administered B16BL6-derived exosomes from the blood circulation in mice. *J Extracell Vesicles*. 2015;4:26238.
48. Zhang G, Huang X, Xiu H, Sun Y, Chen J, Cheng G, et al. Extracellular vesicles: Natural liver-accumulating drug delivery vehicles for the treatment of liver diseases. *J Extracell Vesicles*. 2020;10:e12030.
49. Hecker M, Wagner AH. Transcription factor decoy technology: A therapeutic update. *Biochem Pharmacol*. 2017;144:29-34.
50. Farahmand L, Darvishi B, Majidzadeh-A K. Suppression of chronic inflammation with engineered nanomaterials delivering nuclear factor κ B transcription factor decoy oligodeoxynucleotides. *Drug Deliv*. 2017;24:1249-61.

51. Mehta M, Paudel KR, Shukla SD, Allam VSRR, Kannaujiya VK, Panth N, et al. Recent trends of NF κ B decoy oligodeoxynucleotide-based nanotherapeutics in lung diseases. *J Control Release*. 2021;337:629-44.
52. Li M, Li S, Du C, Zhang Y, Li Y, Chu L, et al. Exosomes from different cells: Characteristics, modifications, and therapeutic applications. *Eur J Med Chem*. 2020;207:112784.
53. Somiya M. Where does the cargo go? Solutions to provide experimental support for the "extracellular vesicle cargo transfer hypothesis". *J Cell Commun Signal*. 2020;14:135-146.
54. Parolini I, Federici C, Raggi C, Lugini L, Palleschi S, De Milito A, et al. Microenvironmental pH is a key factor for exosome traffic in tumor cells. *J Biol Chem*. 2009;284:34211-22.
55. Montecalvo A, Larregina AT, Shufesky WJ, Stolz DB, Sullivan ML, Karlsson JM, et al. Mechanism of transfer of functional microRNAs between mouse dendritic cells via exosomes. *Blood*. 2012;119:756-66.
56. Verweij FJ, Revenu C, Arras G, Dingli F, Loew D, Pegtel DM, et al. Live Tracking of Inter-organ Communication by Endogenous Exosomes *In vivo*. *Dev Cell*. 2019;48:573-589.e4.
57. Yoshimura A, Adachi N, Matsuno H, Kawamata M, Yoshioka Y, Kikuchi H, et al. The Sox2 promoter-driven CD63-GFP transgenic rat model allows tracking of neural stem cell-derived extracellular vesicles. *Dis Model Mech*. 2018;11:dmm028779.
58. Alvarez-Erviti L, Seow Y, Yin H, Betts C, Lakhali S, Wood MJ. Delivery of siRNA to the mouse brain by systemic injection of targeted exosomes. *Nat Biotechnol*. 2011;29:341-5.
59. Zomer A, Maynard C, Verweij FJ, Kamermans A, Schäfer R, Beerling E, et al. *In vivo* imaging reveals extracellular vesicle-mediated phenocopying of metastatic behavior. *Cell*. 2015;161:1046-57.
60. Kamberkar S, LeBleu VS, Sugimoto H, Yang S, Ruivo CF, Melo SA, et al. Exosomes facilitate therapeutic targeting of oncogenic KRAS in pancreatic cancer. *Nature*. 2017;546:498-503.